



Understanding mechanisms of oocyte development by follicular fluid lipidomics

Daniela Antunes Montani¹ · Daniela Paes de Almeida Ferreira Braga^{1,2}  · Edson Borges Jr² · Mariana Camargo¹ · Fernanda Bertuccez Cordeiro^{1,3} · Eduardo Jorge Pilau⁴ · Fábio Cesar Gozzo⁵ · Renato Fraietta¹ · Edson Guimarães Lo Turco¹

Received: 28 November 2018 / Accepted: 22 February 2019 / Published online: 23 April 2019
© Springer Science+Business Media, LLC, part of Springer Nature 2019

Abstract

Purpose The present study aimed to provide a non-invasive approach to studying mechanisms responsible for oocyte development.

Methods To this end, follicular fluid (FF) from 62 patients undergoing in vitro fertilization (IVF) cycles was split into two groups depending on the pregnancy outcome: pregnant ($n = 28$) and non-pregnant ($n = 34$) groups. Data were acquired by the MALDI-TOF mass spectrometry. Principal component analysis (PCA) and orthogonal partial least squares discriminant analysis (OPLS-DA) were applied to the data set. A ROC curve, to predict success rate, was constructed, and the lipids were attributed.

Results Six ions were differentially represented in FF of pregnant and non-pregnant patients, with an area under the curve of 0.962. Phosphatidic acid, phosphatidylglycerol, and triacylglycerol were hyper-represented in the pregnant group, while glucosylceramide was hyper-represented in the non-pregnant group. Enriched functions related to these lipids are steroidogenesis, cellular response, signal transduction, cell cycle, and activation of protein kinase C for the pregnant group and apoptosis inhibition for the non-pregnant group.

Conclusion Human FF fingerprinting can both improve the understanding concerning mechanisms responsible for oocyte development and its effect on embryo implantation potential and assist in the management of IVF cycles.

Keywords Pregnancy · Lipidomics · Follicular fluid · Mass spectrometry · Metabolomics

Introduction

Over the past two decades, the use of assisted reproductive technology (ART) has increased dramatically worldwide.

According to the most recent world report by the International Committee for Monitoring ART, it is estimated that over 237,000 infants were born through ART in a single year, and 1–3% of children born in developed countries are conceived through ART [1].

However, its efficiency in terms of live birth is still low. It was estimated that 4.45 cycles are needed, across all age groups, to achieve one live birth event following an in vitro fertilization (IVF) cycle [2]. Our knowledge of the molecular determinants of embryo viability is poor, and considering that less than 7% of retrieved oocytes develop into a normal embryo that yields a live birth, the understanding of mechanisms affecting cumulus–oocyte complex (COC) interactions may be useful for management of ART cycles.

Human folliculogenesis involves paracrine, autocrine, and endocrine interactions that create an intrafollicular environment for optimal oocyte development. Bidirectional granulosa cells and oocyte signaling via paracrine factors regulates early follicular growth and continuously changes over time to synchronize follicle development with oocyte maturation [3].

✉ Daniela Paes de Almeida Ferreira Braga
dbraga@fertility.com.br

¹ Department of Surgery, Division of Urology, Human Reproduction Section, Sao Paulo Federal University, Rua Embau, 231, CEP: 04039-060 Sao Paulo, SP, Brazil

² Fertility Medical Group, Av. Brigadeiro Luiz Antônio, 4545, CEP: 04511-010 Sao Paulo, SP, Brazil

³ Laboratorio para Investigaciones Biomédicas, Escuela Superior Politécnica del Litoral, ESPOL, Km. 30.5 Via Perimetral, CEP: 09-01-5863 Guayaquil, Ecuador

⁴ Department of Chemistry, Maringá State University, Avenida Colombo, 5790, CEP: 87020-900 Maringá, PR, Brazil

⁵ Institute of Chemistry, University of Campinas, R. Josué de Castro, 126, CEP: 13083-861 Campinas, SP, Brazil

The follicular fluid (FF) is a critical and dynamic component of the ovarian follicle. It enables communication between oocyte and follicular cells, which is required for oocyte development and fertilization competence [4]. Given the importance of the oocyte for ART cycle success, the ovarian cells and the FF have been an area of active research for determining oocyte viability. More recent approaches have focused on the identification of new non-invasive biomarkers of ART success, based on analysis of the oocyte microenvironment [5–8].

The “omics” revolution has stimulated the concept of molecular profiling in biological systems. Despite having already been an intensive area of research in the 1960s [9, 10], lipid research has recently gained prominence with the emergence of lipidomics [11]. Modern approaches for lipidomic analysis are dominated by mass spectrometry (MS) [12], which enables the study of intact lipid molecular species from very small samples [13].

Because of their proximity to the oocyte, FF content may positively correlate with embryo cohort quality. Therefore, the study of signaling molecules, such as lipids, in the FF may provide insight into the follicular environment and improve our understanding of the processes mediated by folliculogenesis and oocyte developmental competence.

In light of this, the goal of the present study was to utilize the analytical power of MS to study the mechanisms responsible for oocyte development, to characterize the lipid profile in the human ovary, and to investigate the relationship between FF lipid content and the reproductive success in patients undergoing IVF cycles.

Materials and methods

Patients

This study included FF samples collected from 62 patients undergoing controlled ovarian stimulation (COS) for ICSI cycles. Samples were split into two groups according to the pregnancy outcome: the pregnant ($n = 28$) and the non-pregnant ($n = 34$) groups.

Patients included in this study met the following inclusion criteria: tubal factor female infertility and/or mild male factor infertility and female age < 36 years.

Written informed consent, in which patients agreed to share the outcomes of their cycles for research purposes, was obtained, and the Institutional Review Board of the São Paulo Federal University Research Ethics Committee approved the study.

Controlled ovarian stimulation

Controlled ovarian stimulation was achieved with a daily dose of recombinant FSH (225 IU/day of Gonal-F, Merck-Serono,

Darmstadt, Germany), starting on day 2 of the cycle. Pituitary blockage was performed with a GnRH antagonist (Cetrorelix; Merck-Serono, Darmstadt, Germany), starting when at least one follicle ≥ 14 mm in diameter was visualized.

Follicular growth was monitored using transvaginal ultrasound examination starting on day 4 of gonadotropin administration. When the leading follicle reached 17 mm in diameter, recombinant hCG (Ovidrel; Serono, Geneva, Switzerland) was administered in order to trigger final follicular maturation. The oocytes were collected 36 h after the administration of hCG through transvaginal ultrasound-guided ovum pick-up.

Preparation of oocytes and intracytoplasmic sperm injection

The retrieved oocytes were incubated in culture medium (SSM Irvine Scientific, Santa Ana, CA, USA) for 3 h. Oocytes that released the first polar body were considered to be matured and were used for ICSI following routine procedures.

Embryo quality, embryo transfer, and pregnancy result

After ICSI, the presumptive embryos were individually maintained in culture media (modified HTF medium with gentamicin–HEPES; Irvine Scientific, Santa Ana, CA, USA) under a humidified atmosphere with 6% CO₂ and 5% O₂ at 37 °C until transfer.

Approximately 18 h after ICSI, fertilization was confirmed by the presence of two pronuclei and the extrusion of the second polar body. Subsequently, embryos were transferred to new drops of culture medium to be cultured individually for 48 h. The quality of the embryos was evaluated under an inverted microscope. On day 3, up to three embryos were transferred. Embryo selection for transfer was based on embryo and oocyte morphology.

Clinical follow-up

Ten days after embryo transfer, the quantitative measurement of serum levels of the beta subunit of human chorionic gonadotropin (β -hCG), which indicates pregnancy, was performed. A clinical pregnancy was defined as the detection of a gestational sac and fetal heartbeat by pelvic transvaginal ultrasonography, performed between 6 and 7 weeks after embryo transfer.

Follicular fluid collection

Follicular fluid was collected by transvaginal ultrasound-guided aspiration, 36 h after hCG administration. The oocyte–cumulus–corona cell complexes were retrieved by using

a stereomicroscope and a glass Pasteur pipette. After this procedure, the follicular fluid that would be discarded was evaluated and only macroscopically clear follicular fluid samples, indicating lack of blood contamination, were included in the study and stored at $-20\text{ }^{\circ}\text{C}$.

When the pregnancy result was obtained, samples from positive and negative groups were pooled together and centrifuged at $800g$ for 10 min. After centrifugation, $50\text{ }\mu\text{L}$ of the supernatant was separated for lipid extraction.

Lipid extraction and mass spectrometry

Lipids were extracted using the method reported by Bligh and Dyer [14] with modifications. Briefly, $50\text{ }\mu\text{L}$ of distilled water was placed in a microtube with $50\text{ }\mu\text{L}$ of the FF sample. Through the addition of $125\text{ }\mu\text{L}$ of chloroform and $250\text{ }\mu\text{L}$ of methanol, the polar and apolar phases were separated. The mixture was vortexed for 1 min, $100\text{ }\mu\text{L}$ of distilled water and $125\text{ }\mu\text{L}$ of chloroform were added, and the samples were centrifuged at $3000\times g$ for 1 min. The lower phase containing the lipids was recovered and transferred to a clean microtube, which was left open overnight at room temperature to evaporate the solvent.

After solvent evaporation, $10\text{ }\mu\text{L}$ of chloroform was added to each sample to dissolve the lipids contained in the microtube. A volume of $2\text{ }\mu\text{L}$ of the extract was deposited onto the well of the mass spectrometer plate and covered with $1\text{ }\mu\text{L}$ of 2,5-dihydroxybenzoic acid (DHB 0.5 M) matrix solution (Sigma-Aldrich, St. Louis, USA) dissolved in 90% methanol.

Mass spectra were acquired in positive-ion mode using a Q-ToF Premier (Synapt HDMS, Waters, Manchester, UK) mass spectrometer (Waters, Manchester, UK) equipped with a 200-Hz solid-state laser in the m/z 700–1200 range in reflectron mode. Typical operating conditions were laser energy 250 a.u. , sample plate 20 V , and trap and transfer collision energies of 6 V and 4 V , respectively (QTOF-MS mode).

Statistical analysis

The mass spectra of each sample were accumulated using MarkerLynx Software 4.1 (Waters, Manchester, UK) and exported to the orthogonal partial least squares discriminant analysis (OPLS-DA) by MarkerLynxTM (Waters, Manchester, UK). The method parameters adopted were as follows: mass tolerance = 0.5, baseline noise = 50, and intensity threshold (count) = 1000 with deisotope data.

The coefficient of correlation vs. variable importance in the projection (VIP) plot of the OPLS-DA analysis provided a list of ions that were differently represented between the groups. These values were used to build a ROC curve and to evaluate the model's potential to predict pregnancy success or failure.

The lipid subclasses of the selected ions were examined using the SimLipid 3.0 software, allowing for H^+ , Na^+ , or K^+ adducts.

Patient and cycle characteristics were analyzed using the SPSS Statistics 21 (IBM, New York, NY, USA) statistical program. Variables were tested for normality and group homogeneity using the Shapiro–Wilk and Levene tests, respectively. When necessary, samples were standardized using z score. Variables were compared between the groups using a Student's t test and were described as mean \pm standard deviation. The considered significance level α was 5%.

In addition, logistic regression analysis was performed using as predictive variables the incidence of the most important ions responsible for group discrimination and patient and cycle characteristics. ROC curves were constructed to evaluate the predictive performances and the area under the curve (AUC) value was calculated for the classification result. The considered significance level of α was also 5%.

Pathway network analysis

The enzymes involved in lipid synthesis were identified using the Kyoto Encyclopedia of Genes and Genomes (KEGG) followed by Protein Knowledgebase (UniProtKB), which was used to identify the protein name. Integrated pathway enrichment analysis of the lipids differentially expressed in the pregnant versus non-pregnant group was performed based on canonical pathways in GeneGoMetaCore 6.15 (Thomson Reuters, St. Joseph, USA). For network analysis, the self-regulation tool was used, and a minimum number of steps were considered; two steps for the pregnant group and five steps for the non-pregnant group.

Results

Cycles and demographic characteristics

Patient and cycle characteristics did not differ among the groups (Table 1).

Follicular fluid lipid composition

Orthogonal partial least squares discriminant analysis (OPLS-DA) was able to clearly distinguish the pregnant and non-pregnant groups (Fig. 1).

Six ions were selected based on their importance in model prediction (variable influence on projection (VIP)), in which three ions were hyper-represented in the pregnant group and three ions hyper-represented in the non-pregnant group (Fig. 2). In the pregnant group, the following lipids were identified: (i) phosphatidic acid (PA; $745.5563\text{ }m/z$), (ii) triacylglycerol (TAG; $773.6153\text{ }m/z$), and (iii) phosphatidylglycerol

Table 1 Patient and cycle characteristics of the pregnant and non-pregnant groups

	Pregnant group (<i>n</i> = 28)	Non-pregnant group (<i>n</i> = 34)	<i>p</i> value
Maternal age	31.43 ± 3.02	29.79 ± 3.65	0.06
FSH (μg mL ⁻¹)	5.83 ± 2.03	6.01 ± 2.03	0.73
Aspirated follicles	14.9 ± 12.4	16.3 ± 9.0	0.732
Retrieved oocytes	9.8 ± 5.3	8.7 ± 5.7	0.345
Fertilization rate (%)	75.1 ± 21.3	73.3 ± 13.0	0.354
High-quality embryo rate (%)	68.9 ± 16.8	64.7 ± 21.3	0.804
Transferred embryos	1.8 ± 0.4	1.8 ± 0.9	0.754
Endometrial thickness (mm)	10.0 ± 1.3	9.7 ± 1.9	0.265

Values described as mean ± standard deviation

(PG; 749.5693 *m/z*). In the non-pregnant group, glucosylceramide (GluCer) (796.6948 *m/z*) was identified in the database, but two other ions, of mass 795.6927 (*m/z*) and 1075.5100 (*m/z*), have not been identified in the available database so far.

Pathway networks

To identify potential pathways and regulatory elements associated with pregnancy, two networks were built *in silico*: the first was constructed using the protein list related to PA, PG, and TAG biosynthesis and the second was built using the protein related to GluCer biosynthesis (Table 2). Both networks were analyzed using the pathway analysis and data mining software MetaCore (GeneGo). Collectively, functional network analysis of the pregnant group showed enrichment in the steroidogenesis process and demonstrated a hypoxic microenvironment (Fig. 3a). Network analysis of the non-pregnant group revealed apoptosis inhibition (Fig. 3b).

Pregnancy prediction model

Logistic regression analysis was performed including the values of ion intensity and clinical data for each sample. The variables contributing to the model were serum FSH on day 3 of the menstrual cycle, the oocyte recovery rate, the MII oocyte rate, the number of transferred embryos, ion 796.6948 (*m/z*), and ion 1075.5104 (*m/z*). The Hosmer and Lemeshow test classified the logistic regression model as well calibrated (*p* = 0.794). These variables were used to build a ROC curve, which presented an AUC of 0.962 (95% confidence interval (CI) 0.919–1.000) (Fig. 3), with a sensitivity and specificity of 0.89 and 0.21, respectively.

Discussion

Follicular fluid, which surrounds the oocyte, is involved in follicular maturation, oocyte growth, and the gradual acquisition of developmental competence [15]. Although intrafollicular factors have been extensively studied during the menstrual cycle, knowledge is still lacking concerning its involvement in the oocyte development process and its possible influence on embryo development competence and implantation.

In fact, biochemical characteristics of FF may provide an important tool for non-invasive assessment of the oocyte. The present study used the MS as an approach to evaluating the lipid profile of FF and identifying lipids associated with successful IVF. To the best of our knowledge, we have provided the most powerful model for the success of infertility treatment to date, with 96.2% accuracy. If used as an adjunct to clinical characteristics, the lipid composition of FF may be a potent tool for infertility treatment management. In addition, based on enzymes involved in the synthesis of the potential lipid biomarkers identified here, we constructed a network pathway that is useful for studying the follicular mechanism involved in oocyte and embryo development.

The pregnant group showed an optimal microenvironment for oocyte development and enhanced steroidogenesis. It was observed by the inhibition of the glucocorticoid receptor alpha (GRα) stimulating phospholipase C (PLC). Recently, it has been demonstrated that GRα may be inhibited by hypoxia with the expression of hypoxia-inducible factor 1-alpha (HIF1α) gene [16]. In fact, the microenvironment during the growth and development of ovarian follicles is poorly oxygenated [17, 18]. This suggests the importance of the preovulatory microenvironment for oocyte development competence.

Diacylglycerol kinase (DAGK) has been described as a ligand for nuclear receptor steroidogenic factor 1 (SF1), which promotes estrogen biosynthesis [19]. Estrogen production by the ovary was also observed to be mediated through the vitamin D receptor (VDR), which is expressed in granulosa cells. It has been suggested that the VDR plays a role in ovary steroidogenesis and in the maintenance of extracellular calcium homeostasis [20]. Concerning the steroidogenic pathway, we also found that phospholipase D2 (PLD2) regulates c-Myc function, which is stimulated by estradiol and gonadotrophins. c-Myc is associated with both proliferating and differentiating events in granulosa cells [21]. It is worth emphasizing that PLC, DAGK, and PLDs are enzymes involved in phosphatidic acid biosynthesis.

It is well known that estradiol plays critical roles in female biology and specifically reproductive function. Intrafollicular estradiol concentrations increased with an increase in follicle diameter [22] and it is involved in the selection of the dominant follicle. It also has a local role in follicular growth, which is consistent with the reported increase in the granulosa cell

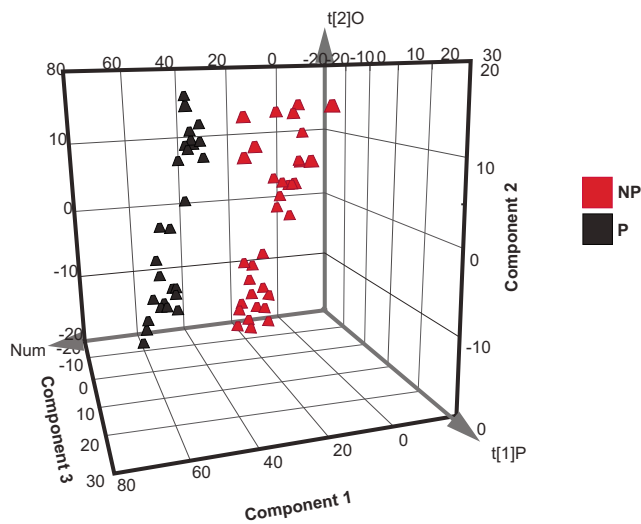


Fig. 1 Principal component analysis (PCA) plot of PC1 vs PC2 vs PC3 for follicular fluid samples from the pregnant group (black points) and from the non-pregnant group (red points)

content of aromatase [23]. Indeed, it has been observed that estradiol promotes development of preantral follicles and stimulates steroidogenesis in granulosa and theca cells in vitro [24]. In addition, it regulates circulating gonadotrophins and synthesis of gonadotrophin receptors, being crucial for the cascade that leads to ovulation [25, 26].

In addition, the role of estradiol on meiosis regulation via the natriuretic peptide precursor C (NPPC)–natriuretic peptide receptor 2 (NPR2) system has been described [27]. The signaling mechanism by which prophase I oocytes are maintained in arrest in vivo has been elucidated, when it was shown that natriuretic peptide precursor C (NPPC) released from mural granulosa cells diffuses through the antral fluid and binds to its receptor, the guanylate cyclase NPR2, located on cumulus granulosa cells [28, 29].

This corroborates our functional regulatory analysis of LPCAT 1, the enzyme that produces phosphatidylglycerol (PG) from Lyso-PG.

Fig. 2 Variable average of VIP ions in both groups is shown in percentage of intensity. NP, non-pregnant group; P, pregnant group; PG, phosphatidylglycerol; PA, phosphatidic acid; TAG, triacylglycerol; GluCer, glucosylceramide. Lipids could not be attributed to the ion masses 795.6927 and 1075.5100

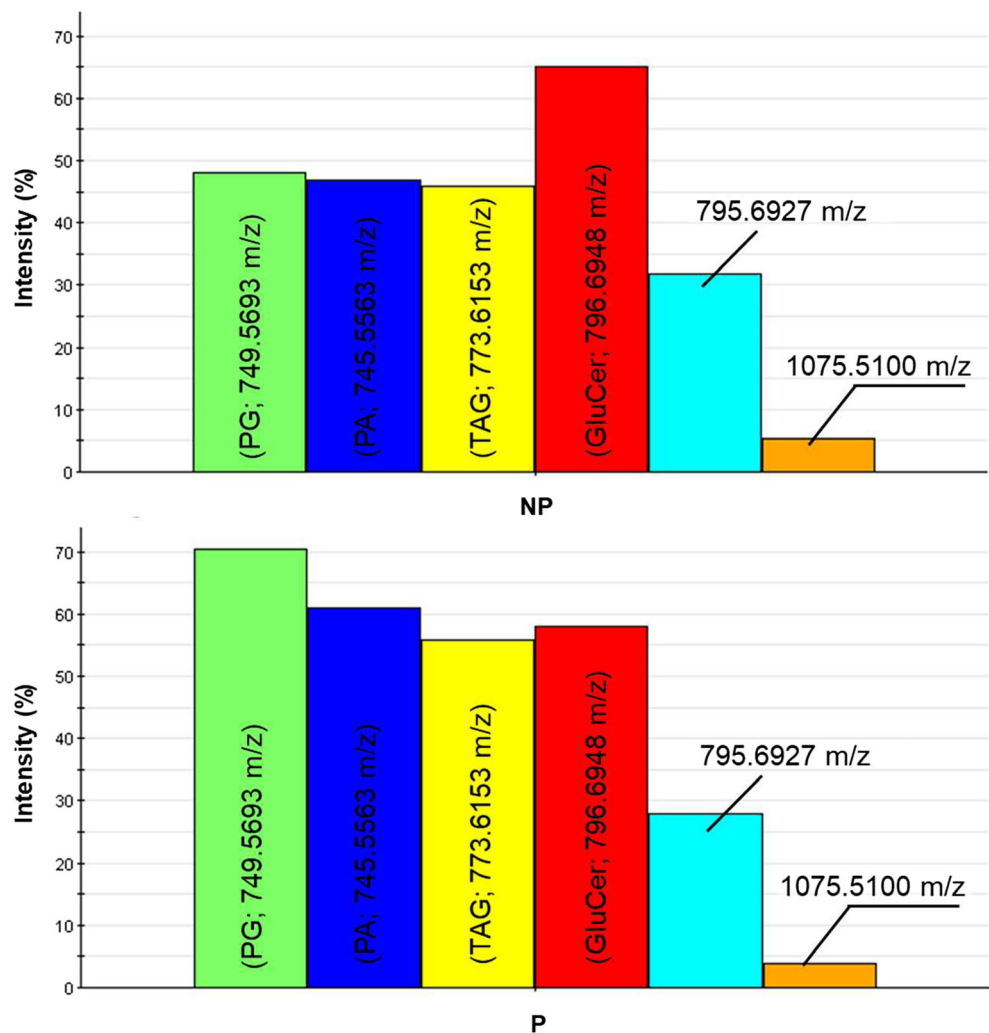


Table 2 Enzymes found to participate in phosphatidic acid, phosphatidylglycerol, triacylglycerol, and glucosylceramide metabolism

Lipid subclass	Protein name	Uniprot ID	Gene	Score	
Phosphatidic acid					
LPA-PA	Glycerol-3-phosphate acyltransferase 3	Q53EU6	AGPAT9	434	
PC-PA	Phospholipase D1	Q13393	PLD1	1074	
	Phospholipase D2	O14939	PLD2	933	
DAG-PA	Diacylglycerol kinase kappa	Q5KSL6	DGKK	1271	
	Diacylglycerol kinase eta	Q86XP1	DGKH	1220	
	Diacylglycerol kinase delta	Q16760	DGKD	1214	
	Diacylglycerol kinase zeta	Q13574	DGKZ	1117	
	Diacylglycerol kinase	Q53SE4	DGKD	1098	
	Diacylglycerol kinase iota	O75912	DGKI	1065	
	Diacylglycerol kinase theta	P52824	DGKQ	942	
	Diacylglycerol kinase beta	Q9Y6T7	DGKB	804	
	Diacylglycerol kinase gamma	P49619	DGKG	791	
	Diacylglycerol kinase alpha	P23743	DGKA	735	
	Diacylglycerol kinase epsilon	P52429	DGKE	567	
	Phosphatidylglycerol (PG)				
	Lyso-PG-PG	Lysophosphatidylcholine acyltransferase 1	Q8NF37	LPCAT1	534
Lysophosphatidylcholine acyltransferase 2		Q7L5N7	LPCAT2	544	
Triacylglycerol (TAG)					
DAG-TAG	Diacylglycerol O-acyltransferase 1	O75907	DGAT1	488	
	Diacylglycerol O-acyltransferase 2	Q96PD7	DGAT2	388	
Glucosylceramide (GluCer)					
Cer-GluCer	Ceramide glucosyltransferase	Q16739	UGCG	394	

We also observed that nuclear factor 4-alpha (HNF4-alpha) induced diglyceride acyltransferase (DGAT1) activity in the pregnant group. There are no reports in the literature regarding the relationship of HNF4-alpha and oocyte development; however, it has been previously described as associated with the transcriptional regulation of genes implicated in glucose metabolism [30]. Although the oocyte has been shown to have a low capacity for glucose metabolism, that of the COC is increased. It allows energy production in the form of ATP and metabolites that can be readily utilized by the oocyte like pyruvate and lactate [31]. Moreover, it is suggested that anionic lipids like PA and PG contribute to glucose transporter (GLUT) activity [32].

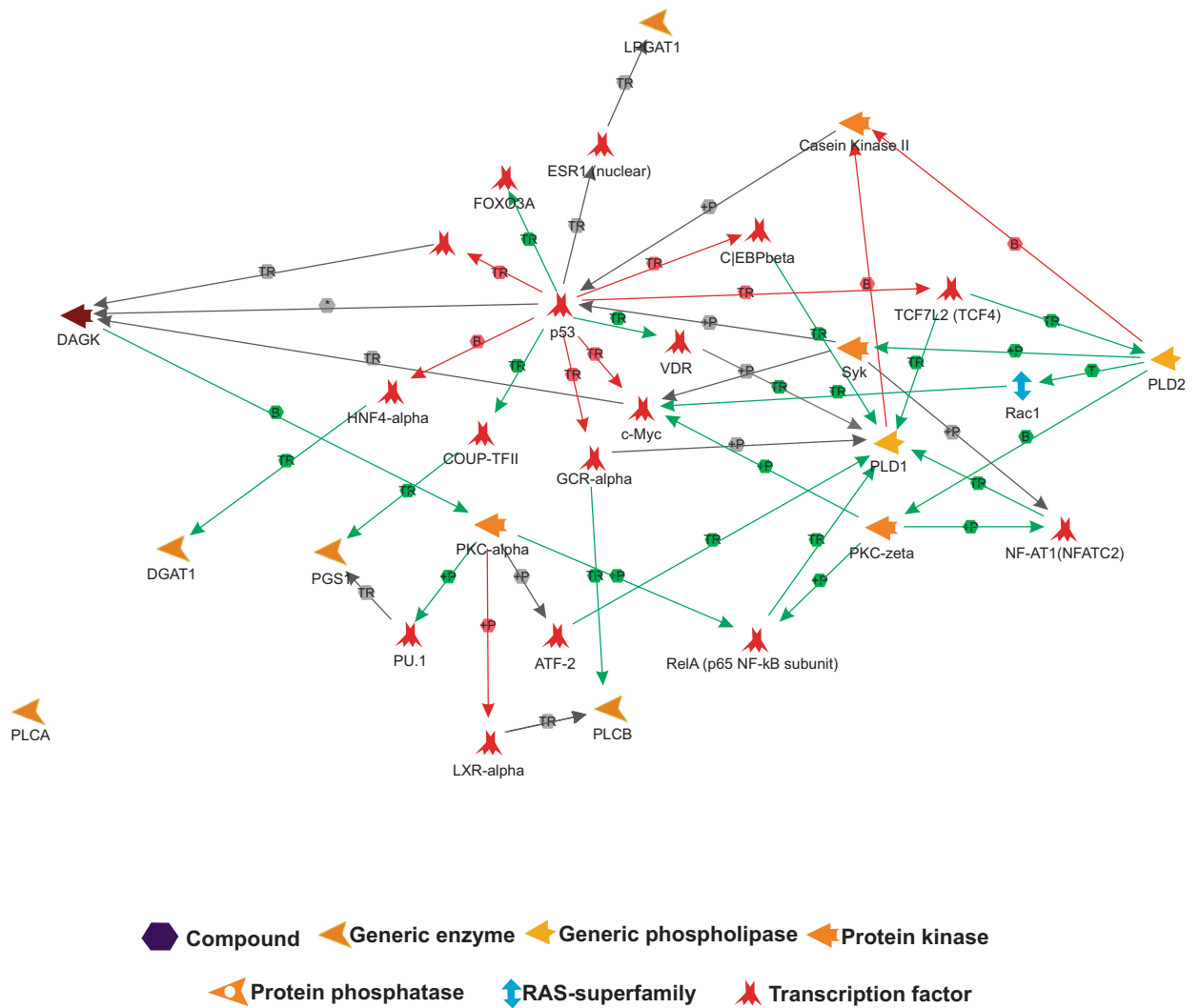
Diglyceride acyltransferase is the enzyme that produces triacylglycerol (TAG), which is responsible for controlling the metabolic flux of fatty acids (FA) into membrane phospholipids and prevents cellular toxicity caused by free FA [33]. In fact, TAG degradation releases metabolites that are critical for efficient cell cycle progression at the G1/S transition [34]. Therefore, it is reasonable that TAG concentration is increased in follicles from high-quality oocytes, leading to embryos with increased developmental competence.

The non-pregnant group showed a possible induction of apoptosis through glucosylceramide transferase, which is encoded by UGCG. GluCer synthesis from cytoplasmic

ceramide occurs through c-Myc, which may be activated or inhibited by PKC-zeta or by protein phosphatase 2A (PP2A), respectively. Ceramide plays a number of physiologic roles that regulate cellular homeostasis [35] and stimulates both PKC-zeta and PP2A for different purposes. The multiple signaling pathways involving PKC-zeta-stimulated ceramide involve suppressing cell growth and ceramide-induced apoptosis [36]. Unlike PKC, PP2A activation may interrupt the principal mechanism of ceramide-induced apoptosis, which occurs through B cell lymphoma 2 (Bcl2) [37].

The glucosylation of ceramide converts it to an inactive form, which modifies the ceramide effector functions [38]. Even though no difference between oocyte maturity was observed between groups, embryo quality was decreased in the non-pregnant group, which may result from poor oogenesis. Moreover, GluCer may be elongated with additional carbohydrates, resulting in a wide variety of glycosphingolipids (GSL) [39], which may be vital for embryo development, mainly during embryo compaction (morula stage) [40]. Unfortunately, in our study, embryo transfer was performed on day 3, before morula formation. Moreover, the presence of GSL and gangliosides was not evaluated because our experiment was carried out in positive ionization mode, while both GSL and gangliosides are ionized in negative ionization mode.

a



b

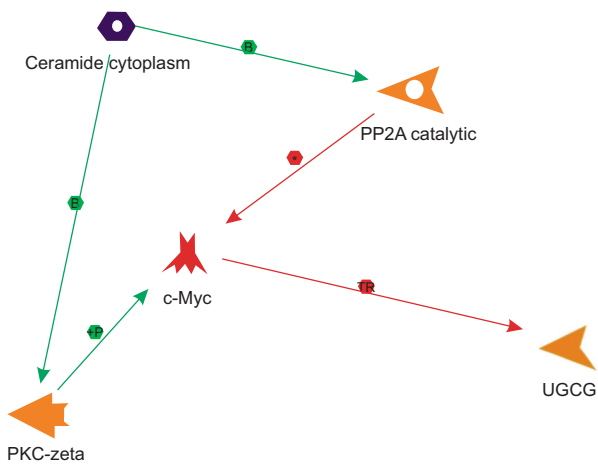


Fig. 3 Significant interaction network analyzed with MetaCore™. The network processes were determined using a self-regulating network algorithm with default settings. Green lines indicate positive regulation, red

lines signify a negative effect, and gray lines represent canonical pathways. **a** Enriched network in the pregnant group. **b** Enriched network in the non-pregnant group

A limitation of the present study was the use of pooled FF samples. In fact, the collection and analysis of individualized samples of follicles adopting single-embryo transfer protocol would be the perfect design. However, even if we used a puncture needle for each follicle, contamination of one sample with another is practically impossible to avoid, and in addition, repeated ovary punctures would cause great discomfort for the patient. Therefore, we hypothesized that the pool of follicular fluid samples would correspond to the ovarian microenvironment that originated the embryo cohort available for transfer.

In summary, the present study revealed the presence of lipids that were differently represented in FF from pregnant and non-pregnant women. Pathway analysis indicated enriched functions related to these lipids, such as steroidogenesis and a hypoxic microenvironment in the pregnant group and apoptosis induction in the non-pregnant group. These findings suggest that lipids in the follicle can be closely correlated with essential functions within the follicular microenvironment. Furthermore, lipid composition of overall FF used as an adjunct to clinical and laboratory data may not only improve our understanding concerning the mechanisms responsible for oocyte development and its effect on embryo implantation but may also be a non-invasive biomarker of follicular cohort competence and embryo implantation potential that could represent a powerful predictive model for pregnancy success.

Funding information The authors wish to acknowledge the Coordination for the Improvement of Higher Education Personnel (CAPES) for providing funding for this research.

Compliance with ethical standards

Ethical Approval The study received approval by the Ethics in Research Committee of Federal University of São Paulo.

Informed Consent All participants included in the study provided the Informed consent form.

Disclaimer The funders had no role in the study design, data collection and analysis, decision to publish, or preparation of the manuscript.

References

- Sullivan EA, Zegers-Hochschild F, Mansour R, Ishihara O, de Mouzon J, Nygren KG, et al. International Committee for Monitoring Assisted Reproductive Technologies (ICMART) world report: assisted reproductive technology 2004. *Hum Reprod.* 2013;28(5):1375–90.
- Sunkara SK, LaMarca A, Polyzos NP, Seed PT, Khalaf Y. Live birth and perinatal outcomes following stimulated and unstimulated IVF: analysis of over two decades of a nationwide data. *Hum Reprod.* 2016;31(10):2261–7.
- Russell DL, Rodgers RJ. Riding the wave: determining the hierarchy of ovarian follicle activation. *Biol Reprod.* 2015;93(4):99.
- Rodgers RJ, Irving-Rodgers HF. Formation of the ovarian follicular antrum and follicular fluid. *Biol Reprod.* 2010;82(6):1021–9.
- Assou S, Haouzi D, Mahmoud K, Aouacheria A, Guillemin Y, Pantesco V, et al. A non-invasive test for assessing embryo potential by gene expression profiles of human cumulus cells: a proof of concept study. *Mol Hum Reprod.* 2008;14(12):711–9.
- Aydiner F, Yetkin CE, Seli E. Perspectives on emerging biomarkers for non-invasive assessment of embryo viability in assisted reproduction. *Curr Mol Med.* 2010;10(2):206–15.
- Uyar A, Torrealday S, Seli E. Cumulus and granulosa cell markers of oocyte and embryo quality. *Fertil Steril.* 2013;99(4):979–97.
- van Loendersloot LL, van Wely M, Limpens J, Bossuyt PM, Repping S, van der Veen F. Predictive factors in in vitro fertilization (IVF): a systematic review and meta-analysis. *Hum Reprod Update.* 2010;16(6):577–89.
- Han X, Gross RW. Shotgun lipidomics: electrospray ionization mass spectrometric analysis and quantitation of cellular lipidomes directly from crude extracts of biological samples. *Mass Spectrom Rev.* 2005;24(3):367–412.
- Oresic M, Hanninen VA, Vidal-Puig A. Lipidomics: a new window to biomedical frontiers. *Trends Biotechnol.* 2008;26(12):647–52.
- Postle AD. Lipidomics. *Curr Opin Clin Nutr Metab Care.* 2012;15(2):127–33.
- Want EJ, Cravatt BF, Siuzdak G. The expanding role of mass spectrometry in metabolite profiling and characterization. *ChemBiochem.* 2005;6(11):1941–51.
- Schwadke D, Oegema J, Burton L, Entchev E, Hannich JT, Ejsing CS, et al. Lipid profiling by multiple precursor and neutral loss scanning driven by the data-dependent acquisition. *Anal Chem.* 2006;78(2):585–95.
- Bligh EG, Dyer WJ. A rapid method of total lipid extraction and purification. *Can J Biochem Physiol.* 1959;37(8):911–7.
- Leroy JL, Vanholder T, Delanghe JR, Opsomer G, Van Soom A, Bols PE, et al. Metabolic changes in follicular fluid of the dominant follicle in high-yielding dairy cows early post partum. *Theriogenology.* 2004;62(6):1131–43.
- Zhang P, Fang L, Wu H, Ding P, Shen Q, Liu R. Down-regulation of GR α expression and inhibition of its nuclear translocation by hypoxia. *Life Sci.* 2016;146:92–9.
- Zhang JY, Diao YF, Oqani RK, Han RX, Jin DI. Effect of endoplasmic reticulum stress on porcine oocyte maturation and parthenogenetic embryonic development in vitro. *Biol Reprod.* 2012;86(4):128.
- Wang J, Qi L, Huang S, Zhou T, Guo Y, Wang G, et al. Quantitative phosphoproteomics analysis reveals a key role of insulin growth factor 1 receptor (IGF1R) tyrosine kinase in human sperm capacitation. *Mol Cell Proteomics.* 2015;14(4):1104–12.
- Mendelson CR, Jiang B, Shelton JM, Richardson JA, Hinshelwood MM. Transcriptional regulation of aromatase in placenta and ovary. *J Steroid Biochem Mol Biol.* 2005;95(1–5):25–33.
- Kinuta K, Tanaka H, Moriwake T, Aya K, Kato S, Seino Y. Vitamin D is an important factor in estrogen biosynthesis of both female and male gonads. *Endocrinology.* 2000;141(4):1317–24.
- Piontkewitz Y, Sundfeldt K, Hedin L. The expression of c-myc during follicular growth and luteal formation in the rat ovary in vivo. *J Endocrinol.* 1997;152(3):395–406.
- Bashir ST, Ishak GM, Gastal MO, Roser JF, Gastal EL. Changes in intrafollicular concentrations of free IGF-1, activin A, inhibin A, VEGF, estradiol, and prolactin before ovulation in mares. *Theriogenology.* 2016;85(8):1491–8.
- Belin F, Goudet G, Duchamp G, Gerard N. Intrafollicular concentrations of steroids and steroidogenic enzymes in relation to follicular development in the mare. *Biol Reprod.* 2000;62(5):1335–43.

24. Rosenfeld CS, Wagner JS, Roberts RM, Lubahn DB. Intraovarian actions of oestrogen. *Reproduction*. 2001;122(2):215–26.
25. Ginther OJ, Gastal EL, Gastal MO, Beg MA. Regulation of circulating gonadotropins by the negative effects of ovarian hormones in mares. *Biol Reprod*. 2005;73(2):315–23.
26. Baerwald AR, Adams GP, Pierson RA. Ovarian antral folliculogenesis during the human menstrual cycle: a review. *Hum Reprod Update*. 2012;18(1):73–91.
27. Zhang M, Su YQ, Sugiura K, Wigglesworth K, Xia G, Eppig JJ. Estradiol promotes and maintains cumulus cell expression of natriuretic peptide receptor 2 (NPR2) and meiotic arrest in mouse oocytes in vitro. *Endocrinology*. 2011;152(11):4377–85.
28. Zhang M, Su YQ, Sugiura K, Xia G, Eppig JJ. Granulosa cell ligand NPPC and its receptor NPR2 maintain meiotic arrest in mouse oocytes. *Science*. 2010;330(6002):366–9.
29. Richard S, Baltz JM. Prophase I arrest of mouse oocytes mediated by natriuretic peptide precursor C requires GJA1 (connexin-43) and GJA4 (connexin-37) gap junctions in the antral follicle and cumulus-oocyte complex. *Biol Reprod*. 2014;90(6):137.
30. Babeu JP, Boudreau F. Hepatocyte nuclear factor 4- α involvement in liver and intestinal inflammatory networks. *World J Gastroenterol*. 2014;20(1):22–30.
31. Harris SE, Leese HJ, Gosden RG, Picton HM. Pyruvate and oxygen consumption throughout the growth and development of murine oocytes. *Mol Reprod Dev*. 2009;76(3):231–8.
32. Hresko RC, Kraft TE, Quigley A, Carpenter EP, Hruz PW. Mammalian glucose transporter activity is dependent upon anionic and conical phospholipids. *J Biol Chem*. 2016;291(33):17271–82.
33. Cnop M, Hannaert JC, Hoorens A, Eizirik DL, Pipeleers DG. Inverse relationship between cytotoxicity of free fatty acids in pancreatic islet cells and cellular triglyceride accumulation. *Diabetes*. 2001;50(8):1771–7.
34. Kurat CF, Wolinski H, Petschnigg J, Kaluarachchi S, Andrews B, Natter K, et al. Cdk1/Cdc28-dependent activation of the major triacylglycerol lipase Tgl4 in yeast links lipolysis to cell-cycle progression. *Mol Cell*. 2009;33(1):53–63.
35. Ruvolo PP. Ceramide regulates cellular homeostasis via diverse stress signaling pathways. *Leukemia*. 2001;15(8):1153–60.
36. Bourbon NA, Yun J, Kester M. Ceramide directly activates protein kinase C zeta to regulate a stress-activated protein kinase signaling complex. *J Biol Chem*. 2000;275(45):35617–23.
37. Ruvolo PP, Clark W, Mumby M, Gao F, May WS. A functional role for the B56 α -subunit of protein phosphatase 2A in ceramide-mediated regulation of Bcl2 phosphorylation status and function. *J Biol Chem*. 2002;277(25):22847–52.
38. Liu YY, Han TY, Giuliano AE, Cabot MC. Expression of glucosylceramide synthase, converting ceramide to glucosylceramide, confers adriamycin resistance in human breast cancer cells. *J Biol Chem*. 1999;274(2):1140–6.
39. Degroote S, Wolthoorn J, van Meer G. The cell biology of glycosphingolipids. *Semin Cell Dev Biol*. 2004;15(4):375–87.
40. Eggens I, Fenderson BA, Toyokuni T, Hakomori S. A role of carbohydrate-carbohydrate interaction in the process of specific cell recognition during embryogenesis and organogenesis: a preliminary note. *Biochem Biophys Res Commun*. 1989;158(3):913–20.

Publisher's note Springer Nature remains neutral with regard to jurisdictional claims in published maps and institutional affiliations.